



Regular Paper

A new large-scale shear apparatus for testing geosynthetics-soil interfaces incorporating thermal condition

Zhiming Chao^{a,b,c,d}, Gary Fowmes^c, Ahmad Mousa^e, Jiaxin Zhou^a, Zengfeng Zhao^f,
Jinhai Zheng^{b,**}, Danda Shi^{a,*}

^a Shanghai Maritime University, Shanghai, 200135, China

^b Hohai University, Nanjing, 211000, China

^c School of Engineering, University of Warwick, Coventry, CV4 7AL, UK

^d Failure Mechanics and Engineering Disaster Prevention, Key Laboratory of Sichuan Province, Sichuan University, Chengdu, 610065, China

^e Department of Civil Engineering, University of Nottingham Ningbo China, Ningbo, 315100, China

^f Wenzhou Jigao Testing Instrument Co., Ltd, Wenzhou, 325000, China



ARTICLE INFO

Keywords:

Temperature-controlled interface shear apparatus
Geosynthetics-soil interface
Monotonic shear test
Cyclic shear test
Creep shear test

ABSTRACT

Geosynthetics-soil interfaces are exposed to varying temperatures coupled with complex stress states. Quantifying the mechanical response of the interface considering this combined influence of temperature and complex stress is always a huge challenge. This study proposes a new displacement and stress-loading static and dynamic shear apparatus that is capable of testing the geosynthetics-soil interfaces with high and low-temperature controlling function. The apparatus satisfactorily simulates monotonic and cyclic direct shear tests, and creep shear tests on geosynthetics-soil interfaces at temperatures ranging from $-30\text{ }^{\circ}\text{C}$ to $200\text{ }^{\circ}\text{C}$. To validate the functionality of this device, a series of temperature-controlled experiments were conducted on different types of interfaces (sand-geogrid interfaces, sand-textured geomembrane interfaces, sand-smooth geomembrane interfaces). The experimental results indicate that the apparatus can simulate static, dynamic, and creep shear loading on geosynthetics-soil interfaces in high and low temperature environments, and these can be measured reliably. It also manifests that temperature has a non-negligible influence on all mechanical interface responses. These findings highlight the significance and potential of the proposed apparatus and its practical implications.

1. Introduction

The current state of practice is to test geosynthetics at constant strain rates, normal stresses, and temperatures (typically around 20°) (Chao et al., 2023b; Ghavam-Nasiri et al., 2019; Morsy et al., 2019; Zeng et al., 2023). While some more specialized equipment exists, most testing is a gross simplification of the real world environment, and there is an urgent need for more sophisticated testing apparatus to be routinely available to allow researchers and practitioners to represent accurately the stress conditions and measure the mechanical evolution rules of geosynthetics interfaces that are subject to the stress history and environmental loadings (Cardile et al., 2021; Xiao et al., 2022; Chao et al., 2024b).

Temperature is an environmental factor that affects the mechanical properties of soil-geosynthetics interfaces (Hanson et al., 2015;

Sudarsanan et al., 2018). Owing to the sensitivity of thermo-softening plastics to changes in temperature, the mechanical parameters of geosynthetics could hugely vary, including stiffness and hardness, which controls the soil-geosynthetics interface behaviour (Liu et al., 2023; Tincopa et al., 2021). This temperature-dependent mechanical response of soil-geosynthetics interfaces has been examined in the existing literature (Bilgin et al., 2021; Frost and Karademir, 2016). For example, Chao and Fowmes, 2022 measured the peak shear strength of clayey soil-geosynthetics drainage layer (GDL) interfaces under different temperatures. The study indicates that with the increase in temperature, the peak shear strength of the interfaces significantly decreases.

2. Motivation and originality

Due to the limitation of the experimental apparatus, the reported

* Corresponding author.

** Corresponding author.

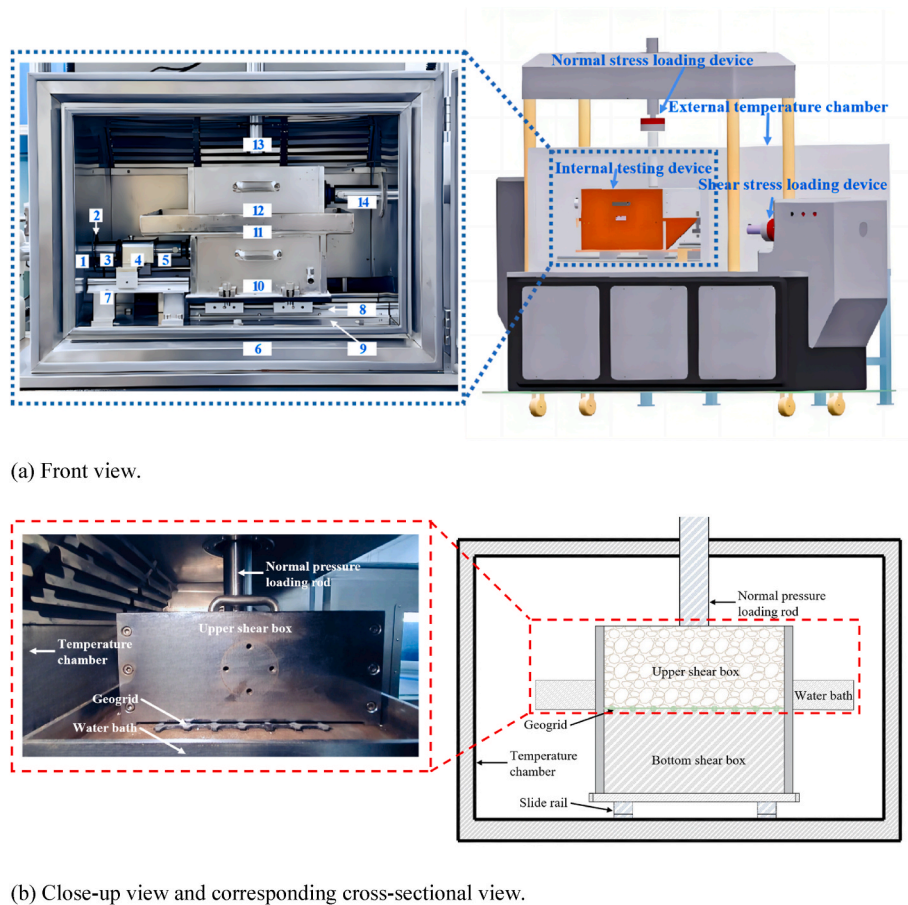
E-mail addresses: zmchao@shmtu.edu.cn (J. Zheng), ddshi@shmtu.edu.cn (D. Shi).

<https://doi.org/10.1016/j.geotexmem.2024.06.002>

Received 18 February 2024; Received in revised form 21 May 2024; Accepted 6 June 2024

Available online 13 June 2024

0266-1144/© 2024 Elsevier Ltd. All rights reserved, including those for text and data mining, AI training, and similar technologies.



(a) Front view.

(b) Close-up view and corresponding cross-sectional view.

Fig. 1. The temperature-controlled large interface dynamic shear apparatus: 1. Shear loading servo control device; 2. Shear load cell; 3. Horizontal steel shear rod; 4. Horizontal sliding block connector; 5. Horizontal displacement sensor; 6. Sliding block; 7. Slide rail; 8. Bottom horizontal support; 9. Slide rail; 10. Bottom shear box; 11. Water bath; 12. Upper shear box; 13. Normal pressure loading rod; 14. Horizontal block rod.

studies/state-of-the-art mainly focus on the mechanical response of soil-geosynthetic interfaces in elevated temperatures (higher than 20 °C) (Chao et al., 2021b, Chao et al., 2021a; Chao et al., 2023; Shi et al., 2023). Conversely, similar studies are very scarce in low temperatures (below freezing), especially when combined with the ability to simulate complex loading conditions and changing interface stress paths. In practical engineering sites, because of seasonal changes and the occurrence of extreme climates, low-temperature conditions are often prevalent in many counties, which poses threats to the serviceability and functionality of the infrastructures utilizing geosynthetics (Chao et al., 2023a, Chao et al., 2024c; Chao et al., 2023a; Han et al., 2013).

Soil-geosynthetic interfaces not only bear monotonic (static) stresses (e.g., overlaying soil layers, surface surcharge) but are also subject to the cyclic stress generated by traffic loading and earthquakes (Hung et al., 2023; Punetha et al., 2019; Zheng et al., 2019). Despite this typical strain-controlled interface, shear testing remains the de facto testing approach. The dynamic mechanical response of soil-geosynthetic interfaces is quiet and has been typically captured using the dynamic direct shear apparatus and the dynamic ring shear apparatus (Chang and Feng (2021); Feng et al. (2021); Liu et al. (2021); Samanta et al. (2022)). (Hou et al., 2022; Tang et al., 2020). Vieira et al. (2013) used the large dynamic direct shear apparatus to carry out displacement and stress-controlled cyclic shear tests on sand-geotextile interfaces, and it indicates that the interface breaks down at lower shear stresses under cyclic stresses, but not under monotonic stresses. Nonetheless, the current devices designed for quantification of the dynamic mechanical response of soil-geosynthetic interfaces are not equipped to alter and control the temperature. As such, there is a

pressing need to design a static and dynamic interface shear apparatus allowing a wide range of temperature-controlling.

The service life of geosynthetics is typically in the order of several decades (Zadehmohamad et al., 2022). Over this rather long service life, and unlike the short-term deformations triggered by the rapidly increasing shear stress, the soil-geosynthetic interfaces usually experience long-term (creep) deformations induced by the constant shear stress (Cardile et al., 2021; Chen et al., 2022; Ghazizadeh and Bareither, 2018). However, the current setups of interface shear apparatus primarily adopt a displacement-controlled loading pattern, which cannot implement creep tests on the interfaces, let alone simulation of the long-term and complex in-situ stresses and environmental conditions (Chao et al., 2023c; Fowmes et al., 2017; Chao et al., 2024a). Combining temperature and load-controlled tests allows the potential for long-term mechanical performance of geosynthetic interfaces to be extrapolated.

There is a need to develop an apparatus that can realistically capture the interface mechanical response between soil and geosynthetics in low and high-temperature environments. In this paper, a bespoke multi-functional soil-geosynthetic interface large direct shear apparatus is introduced. The developed apparatus can conduct both displacement and stress-controlled shear loading as well as static and dynamic shear tests. The mechanical setup is equipped with a temperature-controlling unit (Ranging from −30 °C–200 °C). Using this new apparatus, a series of static, dynamic, and creep shear tests on different types of soil-geosynthetic interfaces under different temperatures were conducted to validate the reliability and stability of the device.

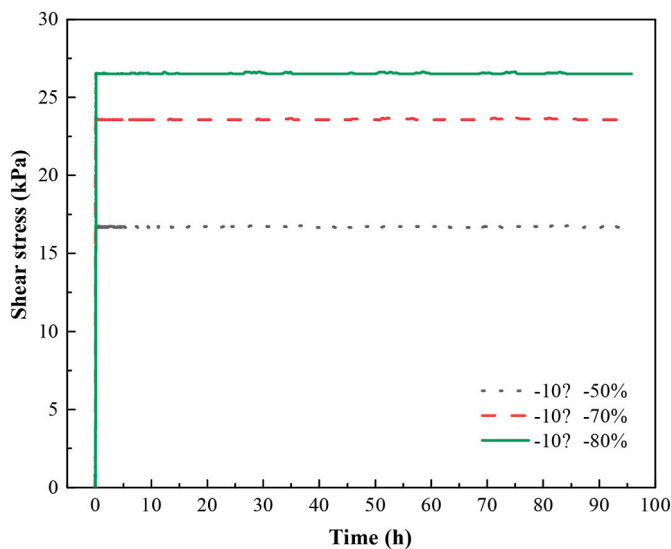


Fig. 2. Shear stress versus elapsed time.

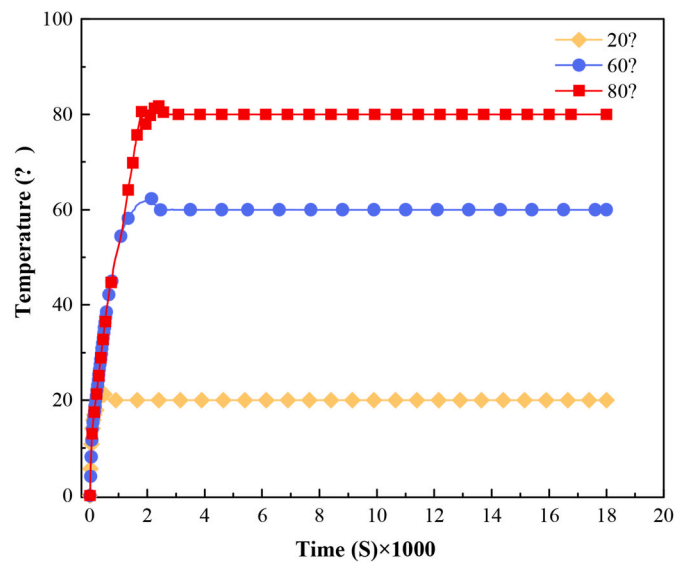
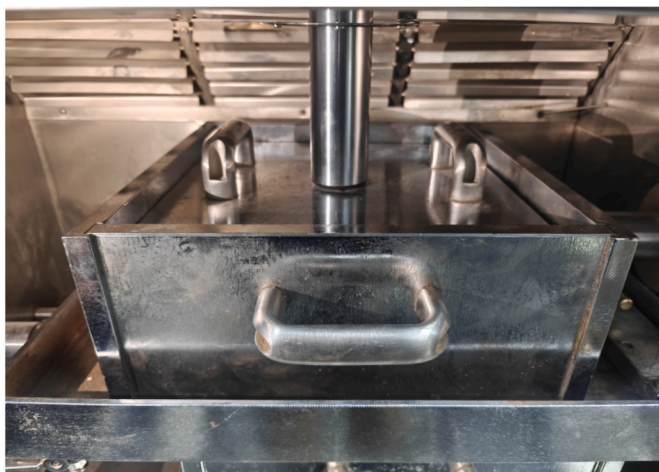


Fig. 4. Chamber temperature versus elapsed time in 7 days.



(a) Before the direct shear tests.



(b) After the direct shear tests.

Fig. 3. The top view images of the loading plate before and after the direct shear tests.

Table 1

The existing study about the temperature-dependent mechanical behaviour of geosynthetic interfaces.

Author	Year	Temperature	Key findings
França et al. (França and Bueno, 2011)	2011	38.1 °C–49.4 °C	Investigation of the temperature effect on the mechanical properties of the sand-biaxial geogrid/woven geotextile/non-woven geotextile interfaces.
Barclay et al. (Barclay and Rayhani, 2013)	2013	22 °C–55 °C	Investigation of the temperature effect on the mechanical properties of sand/clay-geosynthetic clay liner (GCL) interfaces.
Karademir et al. (Karademir and Frost, 2014)	2014	21 °C–50 °C	Investigation of the temperature effect on the shear strength of the soil-geotextile interfaces.
Poggiogalle et al. (Poggiogalle et al., 2018)	2018	–2 °C–35 °C	Investigation of the temperature effect on geosynthetic reinforced soil integrated bridge system (GRS-IBS) abutments.
Ghavam-Nasiria et al. (Ghavam-Nasiria et al., 2019)	2019	20 °C–60 °C	Investigating the dependence of the soil-water characteristic curve (SWCC) of a geosynthetic clay liner (GCL) on temperature and overlying stresses.
Chao et al. (Chao and Fowmes, 2021)	2021	40 °C	Investigating the mechanical properties of the clay-GDL interface under dry-wet cycling, high temperature, and temperature-controlled creep.
Bilgin et al. (Bilgin and Shah, 2021)	2021	3 °C–42 °C	Investigating the temperature effect on the shear strength of soil-geomembrane interfaces.

3. Apparatus

The large interface direct shear apparatus is composed of three main systems (A shear stress loading system, a normal stress loading system, and a temperature controlling system) and a data acquisition and test control system (Fig. 1). All components of the apparatus are produced by

Table 2
The parameters of geosynthetics.

Geosynthetic Type	Parameters	Value
Smooth geomembrane	Thickness (mm)	2.0
	Density (g/cm ³)	0.942
	Fracturing strength (N/mm)	53.5
	Yield strength (N/mm)	29.3
	Yield elongation rate (%)	12
	Fracturing elongation rate (%)	720
Calendared geomembrane (Flat die extruded)	Puncture strength (N)	645
	Thickness (mm)	1.5
	Textured height (mm)	0.26
	Fracturing strength (N/mm)	16.2
	Yield strength (N/mm)	22.3
	Yield elongation rate (%)	12.2
Geogrid	Fracturing elongation rate (%)	120
	Puncture strength (N)	195
	Thickness (mm)	4.02
	Transverse quality control of tensile strength (N/mm)	30
	Longitudinal quality control of tensile strength (N/mm)	30
	Transverse node effectiveness (%)	95
	Longitudinal node effectiveness (%)	95
	Transverse radial stiffness at 0.5% strain (N/mm)	390
	Longitudinal radial stiffness at 0.5% strain (N/mm)	390
	Aperture size (mm)	39 × 39

Table 3
Soil properties of sand.

Parameters	Quartz	Silica
Particle size (mm)	1-2, 2-4	0.075-2
Density (g/cm ³)	2.65	1.50
Optimum water content (%)	9.65	10
Uniformity coefficient	1.45	3.327
Curvature coefficient	0.96	0.3
Median particle size (mm)	1.17, 2.90	0.785

using thermostable materials including cold-resistant rubber and stainless steel, which facilitates the normal operation of the components in high or low-temperature environments. Also, there are thermal insulation dual ring pistons installed in the connections between the environment temperature chamber and horizontal shear steel rod, normal stress loading steel rod, and horizontal block steel rod respectively. The thermal insulation dual ring pistons can prevent from dissipating or entering heat from or into the temperature chamber during the relative movement process between the chamber and rods. The following describes the configurations of the systems.

3.1. Shear stress loading system

The shear loading system is shown in Fig. 1. A servo control system controls horizontal movement, and the other ending is attached to the

Table 4
Test program.

Shear test configurations	Materials	Temperature (°C)	Normal stress (kPa)	Shear amplitude (mm)	Creep shear stresses
Displacement-controlled direct shear test	Silica sand-geogrid interface	-5, 0, 40, 80	50, 150, 250	100	
Stress-controlled direct shear test	Silica sand-textured geomembrane interface	-10, 40, 60	20, 35, 50	100	
Dynamic direct shear test	Silica sand-textured geomembrane interface	-5, 20, 60, 80	20, 35, 50	3	
Creep shear test	Silica sand-textured geomembrane interface	-10, 60	25	100	50%, 70%, and 90% of peak shear strength

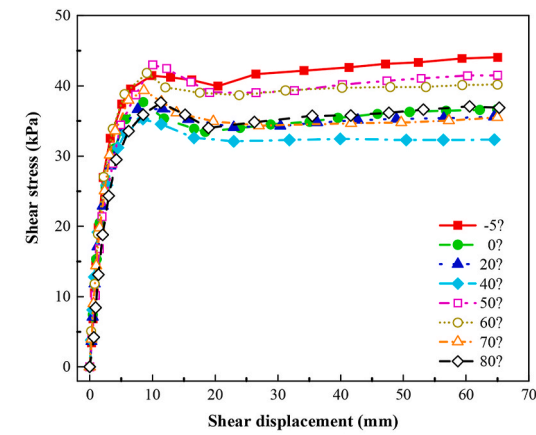
side wall of the bottom shear box. Install a stainless-steel water bath box on the upper surface of the bottom shear box. The top surface of the water bath box is smooth, and the geosynthetic specimen is fixed on the water bath with clamping strips. The upper shear box is placed on top of the water bath, with the geosynthetics sample being fixed underneath. The soil sample is placed into the upper shear box. The loading plate is horizontally placed on the surface of the soil sample, and normal loading is applied using a normal-pressure loading rod. The interface shearing between soil and geosynthetics is conducted by placing soil in the upper shear box and fixing geosynthetics on the top plate of the bottom shear box (The top surface of the water bath). The top surface dimension of the water bath is 400 mm in width and 500 mm in length (Shearing direction), which is larger than the internal dimension of the upper shear box (300 mm in width, 300 mm in length and 200 mm in height). The discrepancy in the dimension can guarantee enough relative interface shear displacement (200 mm) between soil and geosynthetics during shearing. This can be seen in Fig. 1.

During the tests, the shear loading servo control system can impose stress or displacement-controlled shear loading on the bottom shear box through the horizontal shear rod. The displacement-controlled shear loading method involves shearing the soil-geosynthetics interface at a particular displacement rate, with a maximum shear displacement of 200 mm. Comparatively, the stress-controlled shear loading method allows shearing the soil-geosynthetics interface at constant shear stress (creep shear tests) or at a regulated increasing rate, with the maximum shear load of 50 kN. The shear loading servo system can conduct monotonic and cyclic shearing on the interfaces. During monotonic shearing, the upper shear box remains stationary, and the bottom shear box moves along a single direction at a particular displacement rate or stress. For cyclic shearing, the bottom shear box conducts cyclic (alternating) movement along opposite directions of the fixed upper shear box at a prespecified displacement or stress. The new developed apparatus can achieve a certain shear displacement rate in a certain duration. Thus, for certain shear test, the apparatus only can conduct dynamic interface shearing with a constant displacement rate, while for different interface dynamic shear tests, the different displacement rates can be adopted.

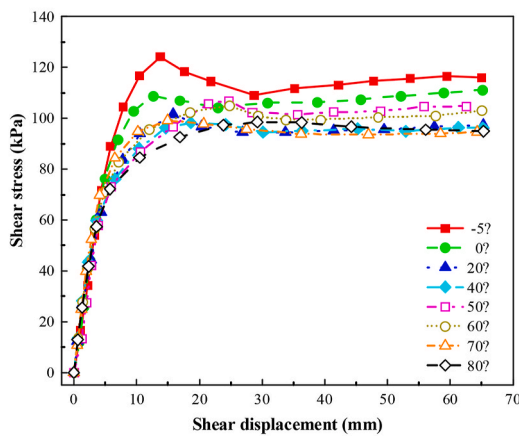
To test the reliability of the shear stress loading system, 50%, 70%, and 80% of the maximum interface shear strength measured in the static direct shear test was applied at the soil-smooth geomembrane interface and stabilized at -10 °C for four days. The measured shear stress is depicted against the elapsed time, as shown in Fig. 2. The shear stress remains stable at the predetermined time of 4 days (5760 min) and a preselected temperature of -10 °C. The maintained constant stress suggests the ability of the system to control the applied shear stress, and the long-term stability of shear stress is evident.

3.2. Normal stress loading system

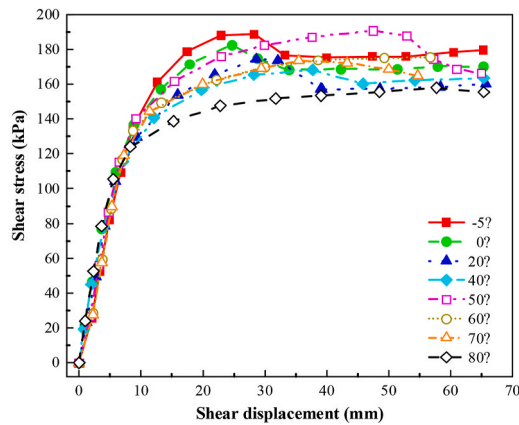
The fixed end of the normal stress loading rod is connected to the normal stress servo-control system. The free end is vertically brought in contact with the loading plate placed above the upper shear box. The normal stress load cell and normal displacement gauge are installed on



(a)



(b)



(c)

Fig. 5. Displacement-controlled direct shear test results at different temperatures: (a) Normal Pressure 50 kPa; (b) Normal Pressure 150 kPa; (c) Normal Pressure 250 kPa.

the loading rod to measure and record the normal stress and vertical displacement of the interfaces during the test, respectively. Similar to the shear stress servo-control system, the normal stress servo-control system can impose normal displacement and stress-controlled loading on the interfaces through the normal stress loading rod, with a maximum imposed displacement of 100 mm and normal stress of 400

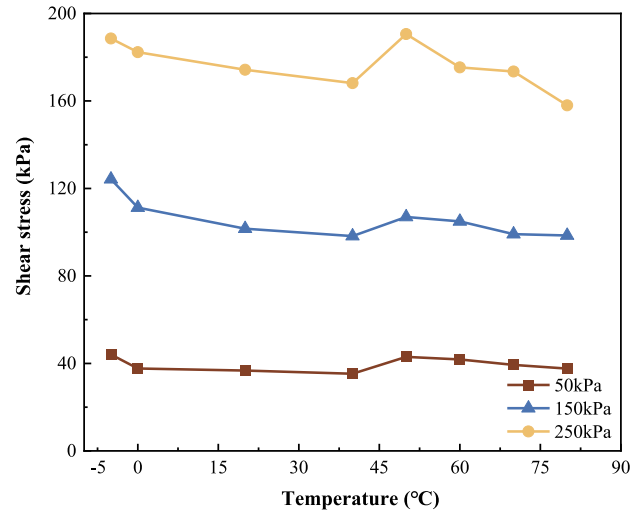


Fig. 6. The relationship curves between peak shear strength and temperature at different normal pressures.

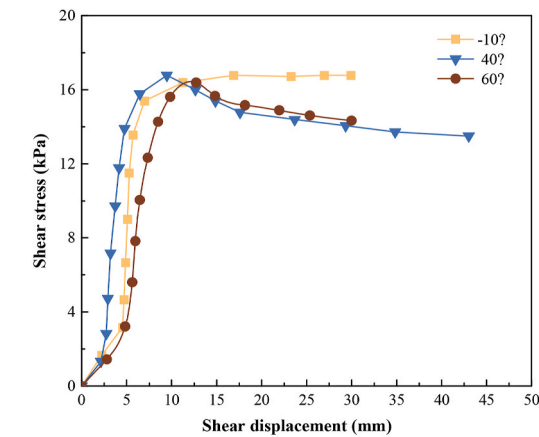
kPa. To avoid the deflection of loading plate during the shearing process, the normal stress loading rod is connected to the loading plate by using screw when designing the apparatus, with the screw installed on the loading plate and threaded hole on the loading rod. It can significantly reduce the deflection of the loading plate during the shearing process to guarantee the accuracy of monitoring normal stress and normal displacement. The top view images of the loading plate before and after the direct shear tests are presented in Fig. 3.

3.3. Temperature-controlling system

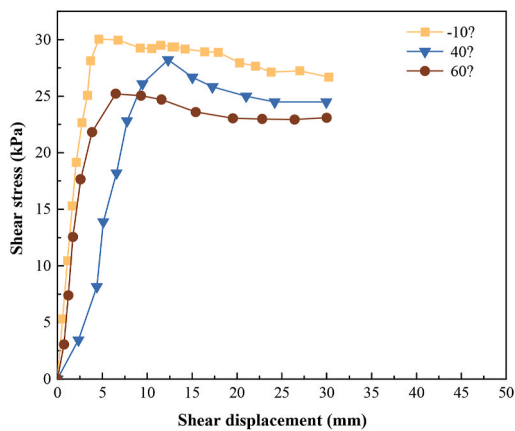
The temperature-controlling system comprises two main components: a large environmental temperature chamber (155 cm in length, 110 cm in width, and 65 cm in height) and an automatic temperature-adjusting system. The ambient temperature chamber is steel that can withstand extremely high and low temperatures. The automatic temperature-controlling system includes an evaporator, a condenser, an expansion valve, a four-way valve, and an air compressor. The primary units of the system are connected through a system of hollow copper tubes filled with a coolant. The evaporator is installed inside the front part of the temperature chamber, with the condenser and air compressor placed inside the rear part.

When the temperature of the environment chamber is elevated, the four-way valve is adopted to reverse the coolant flow direction between the condenser and evaporator. Consequently, the coolant absorbs the heat from the external air and transfers the heat to the inside of the temperature chamber, thereby increasing the temperature of the chamber. When the temperature of the environment chamber is lower than the set test temperature, the temperature-controlling system automatically triggers the heating function; Conversely, when the temperature is higher, the refrigeration function is invoked to reduce the temperature. The automatic temperature-controlling system is capable of adjusting the temperature of the environment chamber at a pre-selected value between $-30\text{ }^{\circ}\text{C}$ and $200\text{ }^{\circ}\text{C} \pm 0.1\text{ }^{\circ}\text{C}$ for seven days, which can cover the temperature variation range of most practical engineering applications. This accurate control warrants testing the soil-geosynthetics interface at the desired temperature. To test the reliability of the high and low temperature-controlling system, the temperature of the environment chamber was set at three different values ($20\text{ }^{\circ}\text{C}$, $60\text{ }^{\circ}\text{C}$, and $80\text{ }^{\circ}\text{C}$) and kept stable for seven days. The temperature of the chamber versus elapsed time is depicted in Fig. 4.

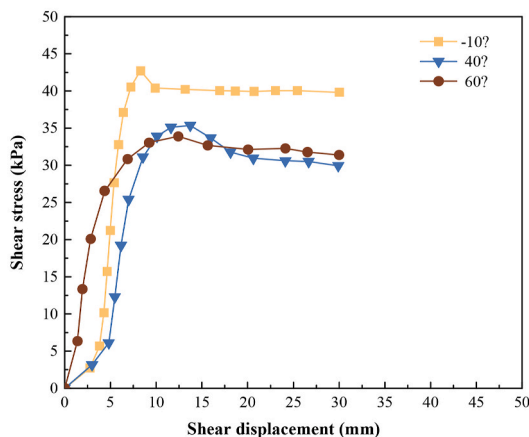
When the experimental temperature is set, the developed apparatus



(a)



(b)



(c)

Fig. 7. Stress-controlled direct shear test results at different temperatures: (a) Normal Pressure 20 kPa; (b) Normal Pressure 35 kPa; (c) Normal Pressure 50 kPa.

can quickly adjust the test temperature to the target value (Within 2000 s, depending on the set temperature). The temperature stabilized during the tests at the target value for a long duration (More than 18,000 s), with minor fluctuations of less than 0.1 °C. This confirms the system’s functionality and the satisfactory level of temperature-controlling. For

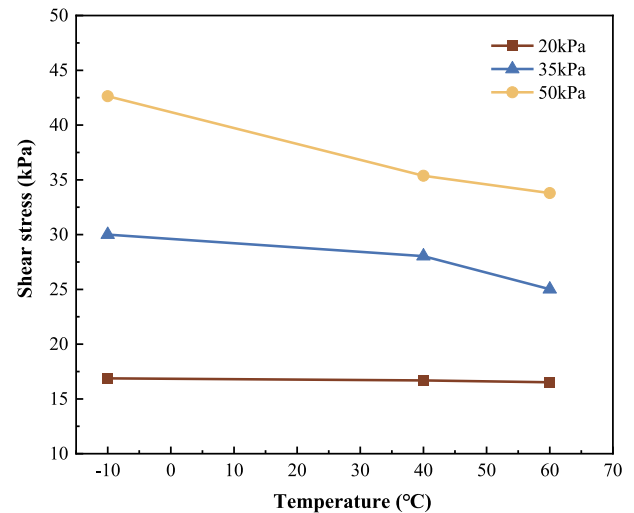


Fig. 8. The relationship curves between peak shear strength and temperature at different normal pressures.

the differences in the temperature between the environmental temperature chamber and the interior of the shear box, in this research, the interface shearing is initiated after the target temperature is kept for 120 min. After testing by adopting a temperature gauge, the interface and soil can reach the target temperature after 120 min in different experimental temperature conditions, and the temperature differences between the environmental temperature chamber and the interior of the shear box can be negligible. For the temperature distribution across the steel and the soil, the designed apparatus controls the temperature of the soil-geosynthetics interface sample by adopting an environmental temperature chamber, which can guarantee the same temperature value inside the entire temperature chamber. It can ensure the even temperature distribution across the steel and the soil. After testing by adopting a temperature gauge, the temperature across the steel and the soil is the same after 120 min in different temperature conditions.

3.4. Data acquisition and test control system

The data acquisition and test control system consists of a horizontal shear displacement LDVT, a shear stress sensor, a temperature transducer, a normal displacement LVDT, a normal stress transducer, a data processor unit, and test control software. The temperature transducer is placed inside the environment temperature chamber to monitor real-time temperature. The shear stress sensor and normal stress transducer are installed inside the horizontal shear rod and normal stress loading rod, respectively. The data processing and test control software has the following functions: (1) Collection and storage of the measured readings; (2) Automatic update and plotting of collected data; (3) Flexible and versatile test parameter setting (Temperature of the chamber, stress or displacement-controlled horizontal shear and vertical loading).

The new apparatus is more advanced and versatile than the available devices that can only heat the geosynthetics-soil interface, but cannot reduce the temperature (Chao et al., 2021a). This new apparatus can conduct interface shear tests within a very wide range of temperatures (−30 °C–200 °C). The current devices utilize a heating plate underneath the interface. In contrast, the new apparatus controls the temperature of the interface by using a sealed temperature chamber, which simulates heat transfer (Ambient temperature) more realistically. Regarding shear stress application, the current devices can impose monotonic shearing on the interface, while the new device can conduct both monotonic and cyclic shearing and creep shear. The versatility of this novel apparatus

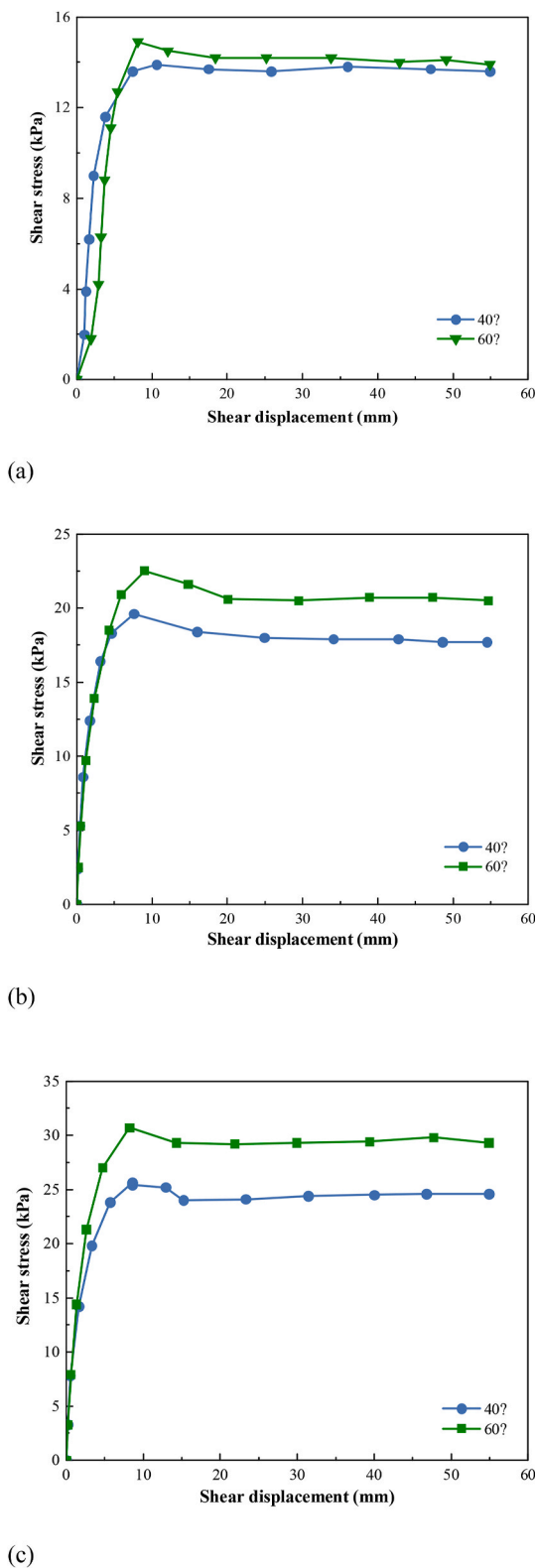


Fig. 9. Displacement-controlled direct shear test results on silica sand-textured geomembrane interfaces at different temperatures: (a) Normal Pressure 20 kPa; (b) Normal Pressure 35 kPa; (c) Normal Pressure 50 kPa.

has never been reported in the literature. The temperature-controlled large dynamic, static and creep soil-geosynthetics interface shear apparatus can investigate the mechanical response of soil-geosynthetics interfaces under the combined effects of thermal and different stress

statuses when simulating the natural engineering environment (see Table 1).

4. Materials and sample preparation

To verify the efficiency of the apparatus, different shear test configurations were conducted on three types of geosynthetics against silica sand: smooth geomembrane, textured geomembrane, and geogrid. The basic properties of the adopted geosynthetics and soil used in the experimental program are shown in Table 2 and Table 3, respectively.

The geosynthetic was cut from a roll (460 mm in length and 280 mm in width) in accordance with ASTM D6072. The cut geosynthetic specimen is fixed to the lower shear box with a clamping bar. The upper shear box was then placed on top of the geosynthetic specimen, with about a 2 mm gap between the upper and bottom shear boxes. The upper shear box was filled with soil in three equal increment layers (25 mm thickness each) at the optimum moisture content and density from the Proctor test. Sixteen times per tamping layer, measured sand samples in the shear box are lightly compacted according to the ASTM specification. Shearing of the soil-geosynthetic interface was induced by the relative sliding of the two halves of the shear box. The shearing rate is test-dependent. Geosynthetics is fixed on the top plate of the bottom shear box, and soil is placed on the upper shear box. For the upper shear box, there are gaps (About 4 mm) in the lower part of its walls that are along the shear direction, which provides space for the passage of geosynthetics with a certain thickness during the shearing process. It avoids the contact between geosynthetics and the walls of the upper shear box, which diminishes the extra resistance during the interface shearing process. For the walls of upper shear box that are vertical to the shear direction, there is no gap in their lower part, which avoids soil leakage.

5. Test configurations and results

This study conducted four different shear test configurations: displacement-controlled direct shear, stress-controlled direct shear, cyclic direct shear, and creep shear tests. The detailed test program is listed in Table 4.

5.1. Temperature and displacement-controlled direct shear test (TDCDST)

The tests were conducted under normal stresses of 50 kPa, 150 kPa, and 250 kPa, simulating a consolidated undrained shear configuration. The test temperature is adjusted at preselected values of $-5\text{ }^{\circ}\text{C}$, $0\text{ }^{\circ}\text{C}$, $40\text{ }^{\circ}\text{C}$, and $80\text{ }^{\circ}\text{C}$. The test was carried on as follows:

- (1) Installing geosynthetics (smooth geomembrane, textured geomembrane, and geogrid) and mounting soil specimen (Silica sand);
- (2) Adjusting the temperature at the preselected value and maintaining it during the test;
- (3) Consolidating the soil-geosynthetics interfaces under the pre-determined normal stress of 25 kPa for 2 h;
- (4) Conducting undrained shearing at the constant displacement shear rate of 1 mm/min along the monotonic direction, with a maximum shear displacement of 100 mm.

The temperature and displacement-controlled direct shear test results of silica sand-geogrid interfaces are presented in Fig. 5.

As shown in Figs. 5 and 6, temperature has a significant influence on the shear stress-displacement relationship. At the same normal stress, the static mechanical response of the interfaces in different temperature environments is different. In general, the peak shear strength of interfaces reduces with the increase in temperature in the range from $-5\text{ }^{\circ}\text{C}$ to $40\text{ }^{\circ}\text{C}$ and $50\text{ }^{\circ}\text{C}$ – $80\text{ }^{\circ}\text{C}$, while the rise in the interface peak strength occurs when temperature rises from $40\text{ }^{\circ}\text{C}$ to $50\text{ }^{\circ}\text{C}$. For

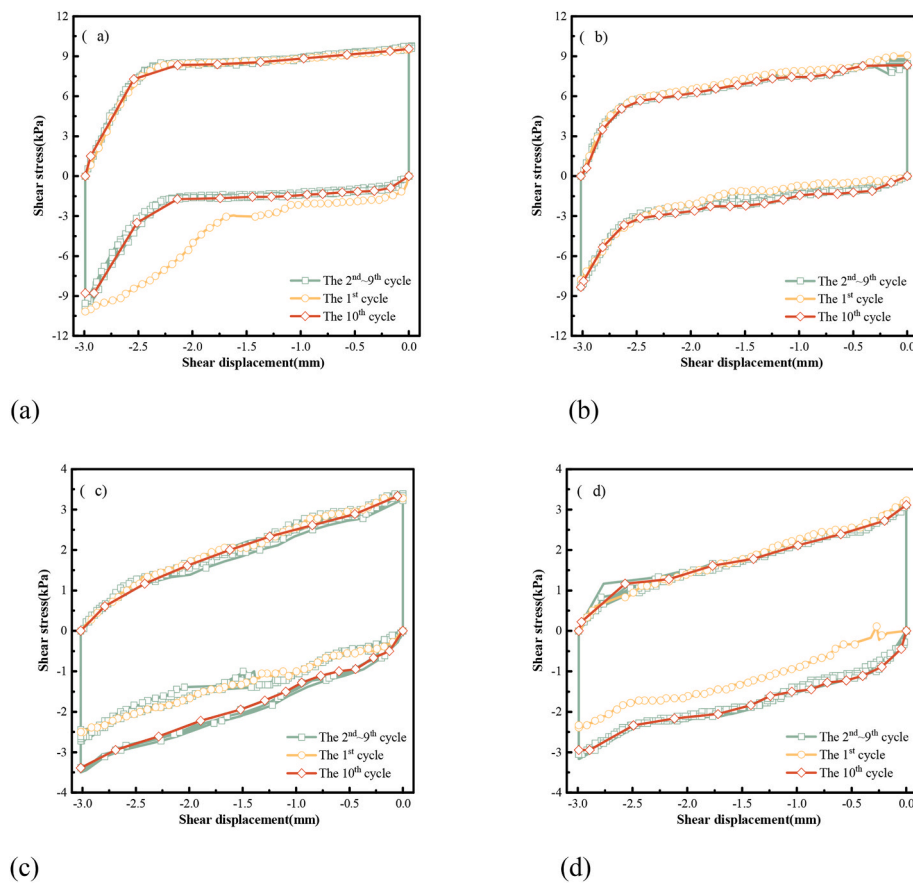


Fig. 10. Temperature-controlled dynamic direct shear test under 20 kPa normal stress: (a) Temperature $-5\text{ }^{\circ}\text{C}$; (b) Temperature $20\text{ }^{\circ}\text{C}$; (c) Temperature $60\text{ }^{\circ}\text{C}$; (d) Temperature $80\text{ }^{\circ}\text{C}$.

example, at normal stress 250 kPa, in $-5\text{ }^{\circ}\text{C}$ the peak shear strength is 190 kPa, while the value for the interface in $20\text{ }^{\circ}\text{C}$ is 172 kPa. The variation rules of interface peak shear strength during the temperature range from $-5\text{ }^{\circ}\text{C}$ to $40\text{ }^{\circ}\text{C}$ and $50\text{ }^{\circ}\text{C}$ – $80\text{ }^{\circ}\text{C}$ are different from that during $40\text{ }^{\circ}\text{C}$ – $50\text{ }^{\circ}\text{C}$ can be attributed to that, the interface interaction can be classified into sliding effects and interlocking effects. In elevated temperature, the softening of geogrid occurs (The hardness of geogrid decreases), which can increase the inserting depth of silica sand particles into geogrid to enhance the interlocking effects. However, the softening geogrid can reduce the friction resistance between silica sand particles and geogrid to weaken sliding effects (Chao et al., 2021a). In the temperature range from $-5\text{ }^{\circ}\text{C}$ to $40\text{ }^{\circ}\text{C}$ and $50\text{ }^{\circ}\text{C}$ – $80\text{ }^{\circ}\text{C}$, the weakening of sliding effects plays the dominating role in the interface interaction, while in the temperature range from $40\text{ }^{\circ}\text{C}$ to $50\text{ }^{\circ}\text{C}$, the enhancement of interlocking effects is the major factor. This results in the rise of interface peak shear strength during the temperature range from $-5\text{ }^{\circ}\text{C}$ to $40\text{ }^{\circ}\text{C}$ and $50\text{ }^{\circ}\text{C}$ – $80\text{ }^{\circ}\text{C}$ and the decrease of interface peak shear strength during the range from $40\text{ }^{\circ}\text{C}$ to $50\text{ }^{\circ}\text{C}$. As with standard shear box tests, the peak and ultimate interface shear strength both increase with the applied normal stress. The significant influence of temperature on the static mechanical response of interfaces indicates temperature dependency. Equally important is the absence or less pronounced peak (Reducing train-softening degree of the interface shear stress-displacement relationship curves) with elevated temperatures (for example at $80\text{ }^{\circ}\text{C}$). Namely, the peak value of shear stress in the relationship curves is less pronounced with the rise of temperature.

5.2. Temperature and stress-controlled direct shear test (TSCDST)

The tests were conducted under normal stresses of 20 kPa, 35 kPa,

and 50 kPa simulating a consolidated undrained shear configuration. Silica sand and textured geomembrane were used in this test. The pre-selected temperatures were $-10\text{ }^{\circ}\text{C}$, $40\text{ }^{\circ}\text{C}$, and $60\text{ }^{\circ}\text{C}$. The test was conducted similarly to the displacement-controlled direct shear except for shearing, which was performed at a constant shear stress rate of 90 N/min along the monotonic direction until a maximum shear displacement of 100 mm was reached. The temperature and stress-controlled direct shear test results are presented in Fig. 7. In this test and as the name implies, the shear stress is controlled rather than the displacement. However, the same trends of TDCDS were observed. As with stress (force) controlled tests, the incremental nature of loading defies capturing smooth/detailed stress-displacement progress.

As shown in Figs. 7 and 8, the shear displacement gradually rises with the increase of shear loading. When shear stress reaches the interface peak shear strength, the large displacement of interfaces suddenly occurs signaling complete interface failure. For the tests at different temperatures, the shear stress-displacement relationship of the interfaces has notable differences. For example, the peak is less pronounced with increasing temperature. In general, the interface shear strength decreases with the rise of temperature. For example, at 50 kPa normal pressure, when temperature increases from $-10\text{ }^{\circ}\text{C}$ to $40\text{ }^{\circ}\text{C}$ and $60\text{ }^{\circ}\text{C}$, the interface shear strength falls by 18.60 % and 23.26 %, respectively. The displacement-controlled direct shear tests on silica sand-textured geomembrane interfaces at temperatures of $40\text{ }^{\circ}\text{C}$ and $60\text{ }^{\circ}\text{C}$ were conducted for comparison (Fig. 9). Figs. 7 and 9 suggest that the observed interface mechanical responses in terms of displacement and stress shear-controlling are comparable. For instance, at a normal pressure of 20 kPa, the interface peak shear strength measured by using displacement and stress-controlled loading methods in the temperatures of $40\text{ }^{\circ}\text{C}$ and $60\text{ }^{\circ}\text{C}$ is 15.24 kPa, and 16.33 kPa, 16.63 kPa, and 17.29

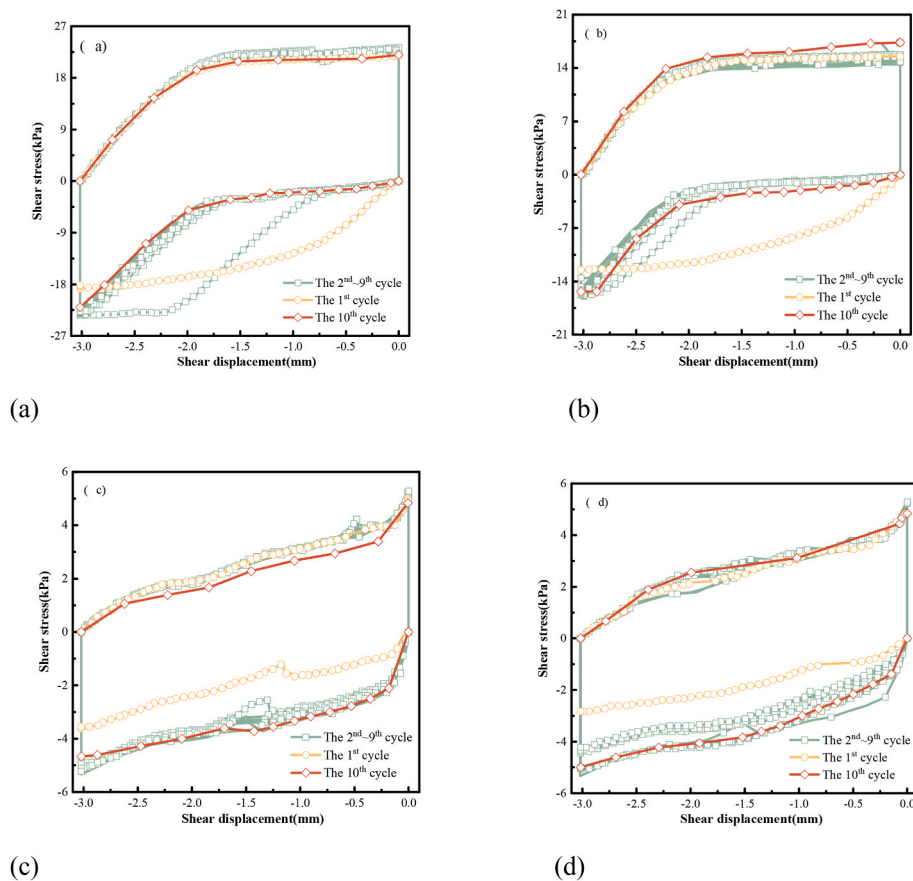


Fig. 11. Temperature-controlled dynamic direct shear test under 35 kPa normal stress: (a) Temperature $-5\text{ }^{\circ}\text{C}$; (b) Temperature $20\text{ }^{\circ}\text{C}$; (c) Temperature $60\text{ }^{\circ}\text{C}$; (d) Temperature $80\text{ }^{\circ}\text{C}$.

kPa, respectively (see Fig. 11).

5.3. Temperature-controlled dynamic direct shear test (TCDST)

Tests were carried out under normal stresses of 20 kPa, 35 kPa, and 50 kPa at five different temperatures of $-5\text{ }^{\circ}\text{C}$, $20\text{ }^{\circ}\text{C}$, $60\text{ }^{\circ}\text{C}$ and $80\text{ }^{\circ}\text{C}$. The test simulated a consolidated undrained shear condition, and a cyclic shear time is 3 min on silica sand-textured geomembrane. Shearing was conducted at a constant shear displacement rate of 1 mm/min until the maximum shear displacement of 3 mm was reached followed by shearing in the opposite direction. The dynamic shear test is terminated when the predetermined cycle time is reached.

The results of temperature-controlled dynamic direct shear tests on silica sand-textured geomembrane interfaces are presented in Fig. 10–Fig. 12.

The observed dynamic mechanical responses significantly vary with changeable temperature and applied normal pressure (Figs. 10–12). It manifests temperature as a key factor that controls the dynamic mechanical properties of the interfaces. To be specific, the relationship curves between shear displacement and stress for the interfaces between silica sand and textured geomembrane all manifests temperature-dependency. In general, the area of the hysteresis loop (The loop formed by the shear stress-displacement curves along opposite shear directions) gradually decreases when the temperature rises from $-5\text{ }^{\circ}\text{C}$ to $60\text{ }^{\circ}\text{C}$. The significant differences between the dynamic mechanical curves of the first cycle and the subsequent cycles can be attributed to the fact that, in the initial status, silica sand sample is relatively loose, which causes the weak interlocking effects between silica sand and geomembrane. After experiencing the first cyclic shear loading, the silica sand sample is compacted, and some silica sand particles are inserted

into the geomembrane, enhancing the interlocking effects between silica sand particles and the geomembrane (Chao et al., 2023). Also, except for the dynamic mechanical properties during the first cyclic shear loading, the mechanical properties during the following cyclic time are close. This is because during the following shear cycles, the silica sand sample is too complex to be further significantly compacted, and the variation in the interlocking effects is relatively marginal (Fowmes et al., 2017). It results in a similar dynamic interface mechanical response during the following shear cycles. The research findings match the existing relevant study outcomes (Chao et al., 2024c).

To quantitatively analyze the impact of temperature on the interface dynamic mechanical characteristics the average value of the maximum shear stress during two opposite shear directions in cyclic shearing processes is determined and identified as the dynamic peak shear strength. The relationship curves between dynamic peak shear strength and temperature at different pressure values are depicted in Fig. 13.

As shown in Fig. 13, the dynamic peak shear strength gradually reduces with the rise of temperature. For example, at normal stress of 20 kPa, when the temperature rises from $5\text{ }^{\circ}\text{C}$ to $20\text{ }^{\circ}\text{C}$ and $40\text{ }^{\circ}\text{C}$, the peak shear strength drops by 14% and 70%, respectively. This indicates the significant undesirable impact of elevated temperature on the dynamic mechanical behavior of interfaces. The decrease of dynamic peak shear strength can be attributed to that, as aforementioned, the interface interaction between soil and geosynthetics can be classified into two different types: Sliding effects and interlocking effects. In elevated temperature, the sliding effects between textured geomembrane and silica sand reduce due to the softening of texture on the surface of geomembrane, while the interlocking effects rise because of the increasing inserting depth of silica sand into geomembrane. For the interface between silica sand and textured geomembrane, sliding effects

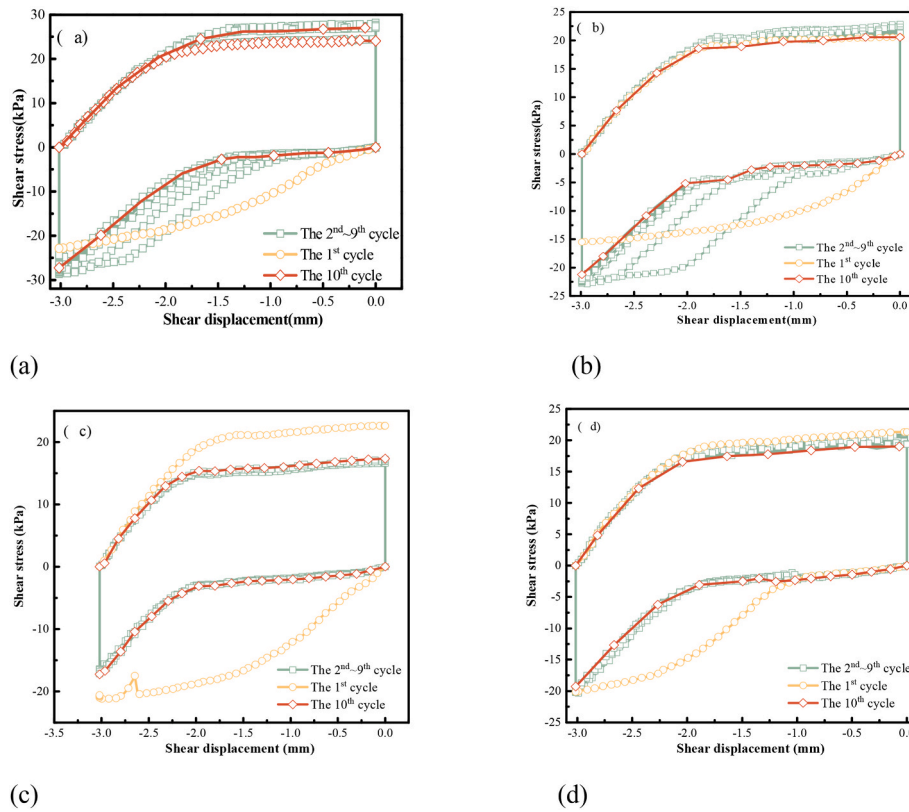


Fig. 12. Temperature-controlled dynamic direct shear test under 50 kPa normal stress: (a)Temperature $-5\text{ }^{\circ}\text{C}$; (b)Temperature $20\text{ }^{\circ}\text{C}$; (c)Temperature $60\text{ }^{\circ}\text{C}$; (d) Temperature $80\text{ }^{\circ}\text{C}$.

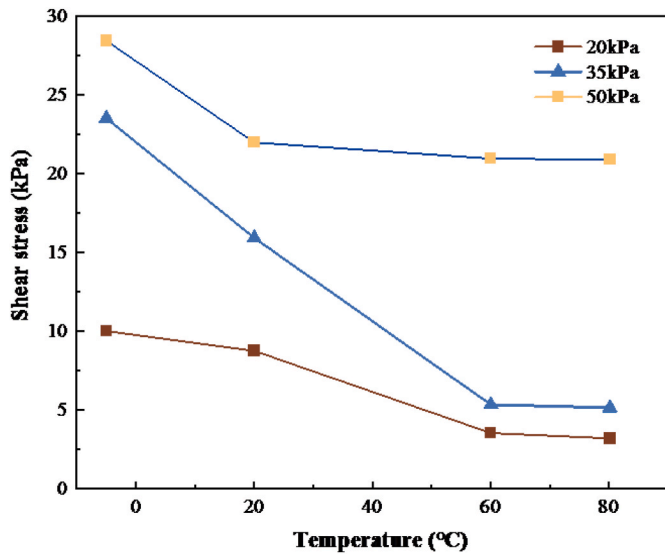


Fig. 13. The relationship curves between dynamic peak shear strength and temperature at different normal pressures.

play a dominant role in the interface dynamic peak shear strength (Chao et al., 2023). Thus, in elevated temperature, the weakening of sliding effects has more significant influence on the dynamic peak strength of silica sand – textured geomembrane interfaces than the enhancement of interlocking effects, which results in the decrease of dynamic peak shear strength in elevated temperature.

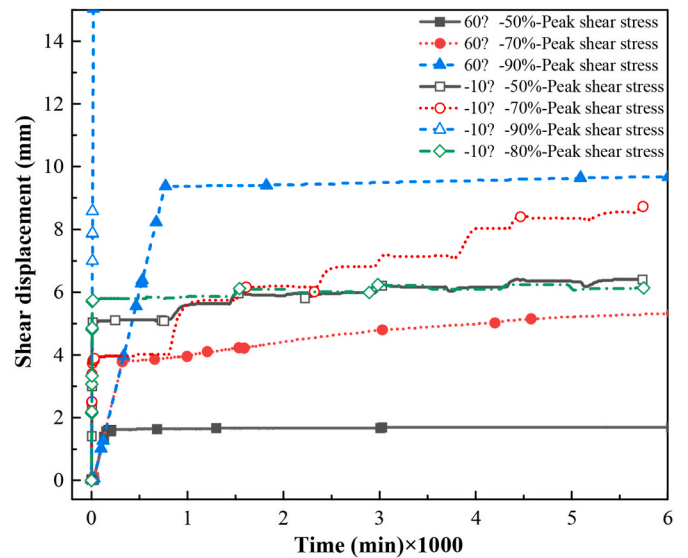


Fig. 14. Temperature-controlled creep shear tests at (a) Temperature $60\text{ }^{\circ}\text{C}$; (b) Temperature $-10\text{ }^{\circ}\text{C}$.

5.4. Temperature-controlled creep shear test (TCGST)

The temperature-controlled creep shear test involves maintaining the shear stress along the soil-geosynthetics interface until failure. When subjected to environmental loadings, the test can replicate the static and dynamic mechanical response of soil-geosynthetics interfaces under in-situ stresses. Creep shearing was performed under 25 kPa normal stress. Three different levels of creep shear stresses were imposed at 50 %, 70

%, and 90 % of the peak interface shear strength. The peak strength is arbitrarily estimated as the average of the maximum shear value from three displacement-controlled direct shear tests. Two extreme temperatures of $-10\text{ }^{\circ}\text{C}$ and $60\text{ }^{\circ}\text{C}$ were adopted for each creep shear stress level. The creep test was conducted on silica sand-textured geomembrane interfaces and is similar to the displacement-controlled direct shear test, except for maintaining the predetermined shear stress on the interfaces throughout the test (The length of the cut geosynthetics is long enough to ensure a constant contact area). The test is terminated when interface failure is reached or else for up to 4 days. The results of the test are presented in Fig. 14.

As shown in Fig. 14, the magnitude of applied creep shear stress affects the mechanical behavior of the interfaces significantly. Also, temperature impacts the creep behavior of the interfaces. Unlike the short-term temperature-dependent interface mechanical properties, the elevated temperature results in a notable decrease in the interface creep shear displacement in the same shearing time. For example, at the creep shear level of 50 % peak shear strength, in the creep stress loading time of the 2000th minute, the interface creep shear displacement at a temperature of $-10\text{ }^{\circ}\text{C}$ is 6.09 mm, which is 143% higher than the creep displacement of 2.5 mm at a temperature of $60\text{ }^{\circ}\text{C}$. This signals a quick interface failure in low-temperature environments as compared to that in a high-temperature environments. For instance, at the creep shear level of 90 % peak shear strength, the interface keeps stable at the temperature of $60\text{ }^{\circ}\text{C}$, while the interface fails abruptly at the temperature of $-10\text{ }^{\circ}\text{C}$. This can be attributed to the fact that the interface creep shear resistance is mainly generated by the interlocking effects between silica sand and geomembrane. In elevated temperatures, the softening of the geomembrane occurs, and silica sand can be inserted into the geomembrane more deeply under the effects of normal stress at high temperature than that at low temperature. It results in that the interlocking effects between silica sand and geomembrane in high temperature are larger than that in low temperature. Namely, the interface creep shear resistance at high temperature is larger than that at low temperature. Thus, the interface is easier to fail in low temperature than that in high temperature. It also indicates temperature variation is evidently a governing factor for the long-term safety and performance of geosynthetics-reinforced or modified soils.

6. Closing thoughts and conclusions

In this research, a new large-scale interface shear apparatus was developed to test the geosynthetics-soil interface mechanical responses under displacement and stress-controlled loading at low and high-temperature environments. The new apparatus is more advanced and versatile than the available devices, which can only heat the geosynthetics-soil interface, but cannot reduce the temperature. This new apparatus can conduct interface shear tests within a wide range of temperatures ($-30\text{ }^{\circ}\text{C}$ – $200\text{ }^{\circ}\text{C}$). In terms of shear stress application, the new device can perform both monotonic and cyclic shearing and creep shearing. The versatility of this novel apparatus has never been reported in the literature.

To validate the functionality of this device, the displacement-loading static direct shear tests, stress-loading static direct shear tests, dynamic direct shear tests, and creep shear tests were conducted on different types of interfaces, including silica sand-geogrid interface, silica sand-textured geomembrane interface, silica sand-smooth geomembrane interface at various temperatures ($-10\text{ }^{\circ}\text{C}$ – $80\text{ }^{\circ}\text{C}$) were implemented. To this end, the device can simulate static (monotonic), cyclic/dynamic, and creep interface shearing in low and high temperatures with satisfactory stability.

The experimental results demonstrate that temperature significantly influences the static, dynamic, and creep mechanical responses of geosynthetics-soil interfaces. Specifically, the peak shear strength of silica sand-geogrid interfaces reduces with the increase of temperature in the static displacement and stress-controlled direct shear tests; The

dynamic peak shear strength of silica sand-textured geomembrane interfaces gradually decreases with the rise of temperature in cyclic direct shear tests; The increase of temperature can result in a notable decrease in the creep displacement under the same creep shear and normal stress in the creep shear tests. These findings highlight the importance of developing this temperature-controlled multi-functional interface shear apparatus.

Notation	
τ	Shear stress
TDCDST	Temperature and displacement-controlled direct shear test
TSCDST	Temperature and stress-controlled direct shear test
TCDST	Temperature-controlled dynamic direct shear test
TCCST	Temperature-controlled creep shear test

CRedit authorship contribution statement

Zhiming Chao: Writing – review & editing, Writing – original draft, Visualization, Supervision, Resources, Project administration, Methodology, Formal analysis, Conceptualization. **Gary Fowmes:** Visualization, Supervision, Investigation, Formal analysis, Conceptualization. **Ahmad Mousa:** Writing – review & editing, Supervision, Formal analysis, Conceptualization. **Jiaxin Zhou:** Writing – review & editing, Validation, Formal analysis, Data curation. **Zengfeng Zhao:** Conceptualization, Methodology, Supervision. **Jinhai Zheng:** Visualization, Resources, Methodology, Data curation. **Danda Shi:** Writing – review & editing, Validation, Supervision, Methodology, Conceptualization.

Data availability

Data will be made available on request.

References

- Barclay, A., Rayhani, M.T., 2013. Effect of temperature on hydration of geosynthetic clay liners in landfills[J]. *Waste Manag. Res.* 31 (3), 265–272.
- Bilgin, Ö., Shah, B., 2021. Temperature influence on high-density polyethylene geomembrane and soil interface shear strength. *J.I.J.o.G., Engineering, G. Int. J. Geosynth. Groun* 7, 1–10.
- Cardile, G., Pisano, M., Recalcati, P., Moraci, N., 2021. A new apparatus for the study of pullout behaviour of soil-geosynthetic interfaces under sustained load over time. *Geotext. Geomembranes* 49, 1519–1528.
- Chang, J.-Y., Feng, S.-J., 2021. Dynamic shear behaviors of textured geomembrane/nonwoven geotextile interface under cyclic loading. *Geotext. Geomembranes* 49, 388–398.
- Chao, Z., Dang, Y., Pan, Y., Wang, F., Wang, M., Zhang, J., Yang, C.J.G.f.E., Environment, t., 2023a. Prediction of the shale gas permeability: a data mining approach. *Geomech. Energy. Envir* 100435.
- Chao, Z., Fowmes, G., 2021. Modified stress and temperature-controlled direct shear apparatus on soil-geosynthetics interfaces. *Geotext. Geomembranes* 49, 825–841.
- Chao, Z., Fowmes, G., 2022. The short-term and creep mechanical behaviour of clayey soil-geocomposite drainage layer interfaces subjected to environmental loadings. *Geotext. Geomembranes* 50, 238–248.
- Chao, Z., Fowmes, G., Dassanayake, S., 2021a. Comparative study of hybrid artificial intelligence approaches for predicting peak shear strength along soil-geocomposite drainage layer interfaces. *Int. J. Geosynth. Groun* 7, 60.
- Chao, Z., Fowmes, G.J.G., *Geomembranes*, 2021b. Modified stress and temperature-controlled direct shear apparatus on soil-geosynthetics interfaces. *Geotext. Geomembranes* 49, 825–841.
- Chao, Z., Li, Z., Dong, Y., Shi, D., Zheng, J., 2024b. Estimating compressive strength of coral sand aggregate concrete in marine environment by combining physical experiments and machine learning-based techniques. *Ocean Eng.* 308, 118320.
- Chao, Z., Shi, D., Fowmes, G., 2023. Mechanical behaviour of soil under drying-wetting cycles and vertical confining pressures. *Environ. Geo.* 40, 1–11. <https://doi.org/10.1016/j.oceaneng.2024.117100>.
- Chao, Z., Shi, D., Fowmes, G., Xu, X., Yue, W., Cui, P., Hu, T., Yang, C., 2023b. Artificial intelligence algorithms for predicting peak shear strength of clayey soil-geomembrane interfaces and experimental validation. *Geotext. Geomembranes* 51, 179–198.
- Chao, Z., Shi, D., Zheng, J., 2024c. Experimental research on temperature-Dependent dynamic interface interaction between marine coral sand and polymer layer. *Ocean Eng.* 297, 117100.
- Chao, Z., Wang, H., Hu, S., et al., 2024a. Permeability and porosity of light-weight concrete with plastic waste aggregate: Experimental study and machine learning modelling [J]. *Construction and Building Materials* 411, 134465.

- Chen, C., Zhu, S., Zhang, G., Morsy, A.M., Zornberg, J.G., Huang, J., 2022. Interface creep behavior of tensioned GFRP tendons embedded in cemented soils. *Geosynth. Int.* 29, 241–253.
- Feng, S.-J., Shi, J.-L., Shen, Y., Chen, H.-X., Chang, J.-Y., 2021. Dynamic shear behavior of GMB/CCL interface under cyclic loading. *Geotext. Geomembranes* 49, 657–668.
- Fowmes, G.J., Dixon, N., Fu, L., Zaharescu, C.A.J.G., 2017. Rapid prototyping of geosynthetic interfaces: investigation of peak strength using direct shear tests. *Geotext. Geomembranes* 45, 674–687.
- Frost, J., Karademir, T.J.G.I., 2016. Shear-induced changes in smooth geomembrane surface topography at different ambient temperatures. *Geosynth. Int.* 23, 113–128.
- Ghavam-Nasiri, A., El-Zein, A., Airey, D., Rowe, R.K.J.G., 2019. Water retention of geosynthetic clay liners: dependence on void ratio and temperature. *Geotext. Geomembranes* 47, 255–268.
- Ghazizadeh, S., Bareither, C.A., 2018. Stress-controlled direct shear testing of geosynthetic clay liners I: apparatus development. *Geotext. Geomembranes* 46, 656–666.
- Han, J., Jiang, Y.J.S.i.C., Regions, A., 2013. Use of geosynthetics for performance enhancement of earth structures in cold regions. *Sci. Cold. Arid. Reg* 5, 517–529.
- Hanson, J., Chrysovergis, T., Yesiller, N., Manheim, D.J.G.I., 2015. Temperature and moisture effects on GCL and textured geomembrane interface shear strength. *Geosynth. Inter* 22, 110–124.
- Hou, R.-Y., Zheng, J.-J., Fang, H., You, L.J.C., 2022. An analytical model for dynamic response of geosynthetic reinforced embankment system under traffic load. *Comput. Geotech.* 142, 104555.
- Hung, W.Y., Nomleni, I.A., Soegianto, D.P., et al., 2023. Centrifuge modeling on the effect of mechanical connection on the dynamic performance of narrow geosynthetic reinforced soil wall[J]. *Geotext. Geomembr.* 51 (4), 156–172.
- Liu, F., Zhu, C., Yuan, G., Wang, J., Gao, Z., Ni, J., 2021. Behaviour evaluation of a gravelly soil-geogrid interface under normal cyclic loading. *Geosynth. Int.* 28, 508–520.
- Liu, H., Han, J., Parsons, R.L.J.A.G., 2023. Numerical analysis of geosynthetics to mitigate seasonal temperature change-induced problems for integral bridge abutment. *Acta Geotech.* 18, 673–693.
- Morsy, A., Zornberg, J., Han, J., Leshchinsky, D.J.G., 2019. A new generation of soil-geosynthetic interaction experimentation. *Geotext. Geomembranes* 47, 459–476.
- Punetha, P., Samanta, M., Mohanty, P., 2019. Evaluation of the dynamic response of geosynthetic interfaces. *Int. J. Phys. Model. Geotech.* 19, 141–153.
- Samanta, M., Bhowmik, R., Khanderi, H., 2022. Laboratory evaluation of dynamic shear response of sand-geomembrane interface. *Geosynth. Int.* 29, 99–112.
- Shi, D., Niu, J., Zhang, J., Chao, Z., Fowmes, G., 2023. Effects of particle breakage on the mechanical characteristics of geogrid-reinforced granular soils under triaxial shear: a DEM investigation. *Geomech. Energy Environ.* 34, 100446.
- Sudarsanan, N., Karpurapu, R., Amrithalingam, V.J.C., Materials, B., 2018. An investigation on the interface bond strength of geosynthetic-reinforced asphalt concrete using Leutner shear test. *Construct. Build. Mater.* 186, 423–437.
- Tang, Y., Xiao, S., Yang, Q.J.A.G., 2020. The behaviour of geosynthetic-reinforced pile foundation under long-term dynamic loads: model tests. *Acta Geotech.* 15, 2205–2225.
- Tincopa, M., Bouazza, A.J.G., 2021. Water retention curves of a geosynthetic clay liner under non-uniform temperature-stress paths. *Geotext. Geomembranes* 49, 1270–1279.
- Vieira, C.S., Lopes, M.d.L., Caldeira, L.M., 2013. Sand-geotextile interface characterisation through monotonic and cyclic direct shear tests. *Geosynth. Int.* 20, 26–38.
- Xiao, S., Zhou, J., Tang, Y., 2022. Centrifuge model test on the behavior of geosynthetic-reinforced pile foundations under simulated train loads. *Acta Geotech.* 17, 4131–4144.
- Zadehmohamad, M., Luo, N., Abu-Farsakh, M., Voyiadjis, G.J.G., 2022. Evaluating long-term benefits of geosynthetics in flexible pavements built over weak subgrades by finite element and Mechanistic-Empirical analyses. *Geotext. Geomembranes* 50, 455–469.
- Zeng, W.-x., Ying, M.-j., Liu, F.-y.J.T.G., 2023. Investigation on the cyclic shear response of stereoscopic geogrid-reinforced coarse-grained soil interface. *Transp. Geotech* 38, 100905.
- Zheng, Y., McCartney, J.S., Shing, P.B., Fox, P.J., 2019. Physical model tests of half-scale geosynthetic reinforced soil bridge abutments. II: dynamic loading. *J. Geotech. Geoenviron* 145, 04019095.